



NOVA

University of Newcastle Research Online

nova.newcastle.edu.au

Khan, Reduan H.; Ustun, Taha Selim; Khan, Jamil Y. "Differential protection of microgrids over a WiMAX network" Published in Proceedings of the 2013 IEEE International Conference on Smart Grid Communications, p. 732-737, (2013)

Available from: <http://dx.doi.org/10.1109/SmartGridComm.2013.6688046>

© 2013 IEEE. Personal use of this material is permitted. Permission from IEEE must be obtained for all other uses, in any current or future media, including reprinting/republishing this material for advertising or promotional purposes, creating new collective works, for resale or redistribution to servers or lists, or reuse of any copyrighted component of this work in other works.

Accessed from: <http://hdl.handle.net/1959.13/1335720>

Differential Protection of Microgrids over a WiMAX Network

Reduan H. Khan*, Taha Selim Ustun[†], and Jamil Y. Khan*

*School of EECS, The University of Newcastle, NSW 2308, Australia.

[†]Department of ECE, Carnegie Mellon University, PA 15213, United States.

Abstract—One of the widely used methods for protecting power system elements is the Line Current Differential Protection (LCDP) schemes that works by comparing the vector difference between the measured currents at two or more line-terminals. Communications network plays a vital role in such schemes since the local and the remote line-terminals must exchange their current elements to perform the differential calculation. This paper investigates the use of an IEEE 802.16/WiMAX based wide-area wireless communications network to support LCDP schemes in the smart microgrids. The possible use of the WiMAX network as a synchronization source to the differential relays is also proposed. Using theoretical capacity analysis, the paper examines the use of advanced WiMAX features such as persistent scheduling, robust header compression and grant synchronization to efficiently support such a scheme. In addition, simulations were conducted using an OPNET simulation model to analyze the communications performance of the scheme in terms of packet-loss and delay. The results indicate that a WiMAX network along with its advanced features is particularly well-suited to meet the challenging requirements of a differential protection scheme.

I. INTRODUCTION

For almost a century, the Line Current Differential Protection (LCDP) schemes are being widely used for protecting power system elements such as generators, transformers and transmission lines. They are well-regarded for their high selectivity and sensitivity with a very low configuration complexity[1]. A LCDP relay works by continuously measuring its local line-current and comparing it to that of a remote terminal to detect a vector difference in current. If the difference exceeds a certain threshold, a fault is detected and the relay operates. Communications network plays a vital role in such a scheme since the local and the remote line terminals must exchange their current elements to perform the differential calculation.

In recent times, the advent of microprocessor based digital relaying techniques has renewed the potential of LCDP schemes, especially in context of the next-generation smart grid networks. One such promising application area is envisaged to be in protecting the microgrids. Although the use of LCDP schemes in microgrids has been proposed and investigated in several works[2], [3], the communication challenges of such a scheme were not fully addressed.

Typically the LCDP schemes are designed to support either two or three terminal feeders. However, in microgrids the direction and amount of fault-current may change rapidly due

to the time varying load-supply profile. This requires a multi-terminal LCDP scheme where they relays need to communicate with each other either directly or via an intermediate node[3]. Besides, the line current measurements need to be precisely synchronized so that they can be evenly compared. Otherwise, the synchronization error will result in phase angle offset and lead to error in differential current calculation[4]. Above all, a reliable communications network is a must to facilitate continuous exchange of real-time measurements among the relays.

In this paper, we investigate the use of an IEEE 802.16/WiMAX based wide-area wireless communications network to support LCDP schemes in the smart microgrids. In particular, we concentrate on the Radio Resource Management (RRM) issues to transfer the real-time line current measurements among the differential relays. In addition, we propose the possible use of a Time Division Duplex (TDD) based WiMAX network as a synchronization source to the relays[5]. We discuss some of the advanced WiMAX features such as persistent scheduling, Robust Header Compression (ROHC), and grant synchronization that can be used to support LCDP schemes more efficiently. Using theoretical capacity analysis, we examine the effect of these features on the overall capacity and utilization of the WiMAX network. Moreover, using a discrete event simulation model based on OPNET, we examine the delay and packet-loss performance of the WiMAX network under a LCDP scheme.

The rest of the paper is organized as follows. Section II briefly describes a generic LCDP scheme and outlines its key communications requirements. Section III discusses the possible use of the IEEE 802.16/WiMAX standard for supporting such schemes and highlights the key challenges such as synchronization, radio resource allocation, and packet-loss and retransmission. Capacity and performance analyses of the WiMAX network for the generic LCDP scheme are presented in Section IV and V respectively. Finally, section VI concludes the paper.

II. DIFFERENTIAL PROTECTION OVERVIEW

The LCDP schemes works by the principle of Kirchhoff's current law i.e. under all circumstances the vector sum of all the currents in a protection zone will add up to zero. Fig. 1 shows a generic LCDP scheme with two line terminals. Both of the relays at the end of the protected line are continuously exchanging their line current elements I_1 and I_2 via the

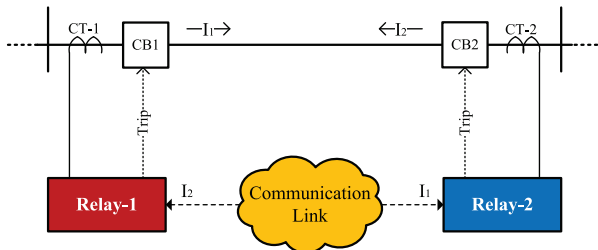


Figure 1: A generic LCDP scheme for a two-terminal feeder.

communications link. Under normal circumstances, the sum of these current elements at each relay should be zero. Should there be a fault, the relays will detect a differential current component $I_D = |I_1 + I_2|$ and therefore, trip the associated circuit breaker (CB). Note that in practice, the vector sum of the currents might not always be zero due to measurement errors. Therefore, a *Restrained Current* is used to compensate for such an error which is typically a function of the individual current magnitudes of the relays i.e. $I_R = f(|I_1|, |I_2|)$. In case $I_D > I_R$, the relay operates.

In case of a multi-terminal LCDP scheme, all the relays under the same protection zone need to share their current elements with each other. This can be done by using either direct point-to-point communications links among the relays or a multiplexed channel with one or more intermediate nodes. In such a case, the differential current and restrained current can be calculated using the *Alpha Plane* concept. For more details, the interested readers are referred to [6].

In most of the modern LCDP schemes, the current elements are exchanged either as digitized samples of the analog current or as current phasors with magnitude and phase angle[2]. If current samples are used, synchronization is typically provided by measuring the round-trip delay of the communications channel and then shifting the phase angle of the measured current accordingly[4]. In contrast, the phasor measurements are time-stamped using a common timing reference such as GPS (Global Positioning System) that eliminates the requirement for a channel-based synchronization technique[7]. Moreover, phasor data communication is regulated by international standards such as IEEE C37.118.2-2011 and IEC61850-90-5 that allow the use of commercially available IP (Internet Protocol) and Ethernet based networks. Hence, phasor based LCDP schemes are expected to be the prevailing one for the next-generation smart grid.

For this study, we consider a phasor-based LCDP scheme over a WiMAX network. Fig. 2 shows the MPDU (*MAC Protocol Data Unit*) structure the current phasor data packet comprised of a measurement payload and lower layer protocol overheads such as UDP (User Datagram Protocol) and IP headers, WiMAX MAC header, and CRC (Cyclic Redundancy Check) bits. The current measurement payload is comprised of 4 fields. The first two fields are used to identify the individual relay station and its protection zone, followed by a time-tag field and the current phasor readings (3 phasors for a 3 phase line). The field sizes are set according to the IEEE C37.118.2 standard[8].

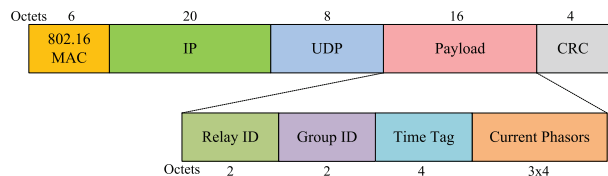


Figure 2: MPDU structure of a current phasor data packet over WiMAX.

From a communications network's perspective, the key requirement here is to transfer the real-time line-current measurements (i.e. the current phasors) reliably within a specific delay bound. The overall communications load from a differential relay depends on two factors – the total size of the measurement packet and the rate of measurement. Although a higher measurement rate may allow a faster response, it comes at the cost of a higher communications load. Nonetheless, while a high voltage transmission feeder requires a high measurement rate (e.g. 2-4 measurements per cycle), the requirements can be slightly relaxed for a distribution feeder considering the relative impacts of an outage. Since the focus of this paper is to protect the microgrids which are typically located in the distribution grid, we assume a maximum delay bound of 1 cycle (20 ms considering 50 Hz power systems) for the communications network.

III. DIFFERENTIAL PROTECTION OVER WiMAX

In this section, we discuss how a differential protection scheme can be implemented over a WiMAX network and the additional WiMAX features that can be used to support it more efficiently.

A. Synchronization

A typical TDD based WiMAX network requires precise synchronization and timing to assure that the Subscriber Stations (SSs) are able to access their Uplink (UL) and Downlink (DL) time-slots without interfering with each other. Typically, a WiMAX Base Station (BS) receives synchronization information either directly from a GPS receiver or from a master clock in the IP backbone network using the IEEE1588 based Precision Time Protocol (PTP). The reference time tolerance specified in the IEEE 802.16-2009 standard is $\pm(T_b/32)/4$ where T_b is the OFDM symbol time ($\sim 91.4 \mu\text{s}$)[5]. This yields a timing error tolerance of $\pm 0.714 \mu\text{s}$.

When a SS performs network entry, it firsts synchronizes itself with the DL preamble transmitted at the beginning of each WiMAX frame (see Fig. 3). However, synchronizing with the DL preamble does not guarantee precise time synchronization with the BS. This is because, the SS are placed at random locations within the BS's coverage area and their signal arrival times depend on their relative distance from the BS. Therefore, the next level of synchronization is obtained by the ranging process. Ranging adjusts each SS's timing-offset such that it appears to be co-located with the BS. The BS calculates the amount of timing offsets based on the round-trip delay between itself and the SS.

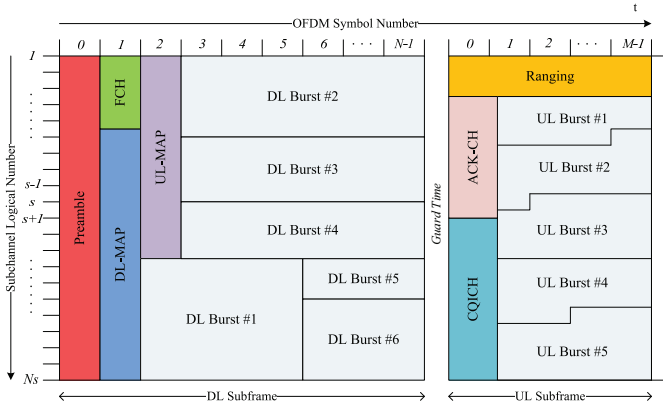


Figure 3: The frame structure of a OFDMA/TDD WiMAX System[5].

The IEEE C37.188.2 standard for synchrophasor measurement allows a Total Vector Error (TVE) of 1% that corresponds to a time error of $\pm 31 \mu\text{s}$ for a 50 Hz power system[8]. This is well below the synchronization requirement of the WiMAX stations (i.e. $\pm 0.714 \mu\text{s}$). Therefore, a WiMAX network is able to provide adequate synchronization to the phasor based differential relays. This removes the need of installing a separate GPS receiver for the relays which may significantly reduce the deployment cost of a LCDP scheme.

B. Radio Resource Management

Although the LCDP schemes require peer-to-peer communication among the relays, in a cellular wireless environment like that of WiMAX, all the data packets have to traverse via the BS. This eliminates the requirement of mesh connections (i.e. $n-1$ links for each of the n relays) by proving a central point of communication. Here, the BS will forward the incoming data packets to the destination relay(s) based on their destination IP addresses. Thus, each current measurement data packet is associated with an UL component i.e. from the source relay to the BS and a DL component i.e. from the BS to the destination relay.

Note that for a WiMAX network, the multi-terminal LCDP scheme can be considered as a special case of the two-terminal scheme where the BS multicasts the DL component to all the member relays within a protection zone.

The radio resource allocation in a WiMAX network is based on a request/grant mechanism where each SS is required to reserve a sufficient amount of bandwidth from the BS before any data transmission. Fig. 3 shows the frame structure of a TDD, OFDMA (Orthogonal Frequency Division Multiple Access) based WiMAX system. As seen from the figure, the DL subframe contains the DL and UL MAP (Medium Access Protocol) signaling messages that are used to provide radio resource allocations over the DL and the UL subframes. Each Information Element (IE) in the MAP messages indicates the start time and the OFDMA channel details of an UL/DL data burst.

To facilitate radio resource sharing among different users, the IEEE 802.16 standard provides three mechanisms – con-

tention based Best-Effort (BE) service, the contention free Polling Service (PS), and reservation based Unsolicited Grant Service (UGS)[5]. In [9], the authors have investigated the performance of these scheduling services for synchrophasor data communication and concluded that the UGS provides the best performance in terms of delay and radio resource usage.

Under UGS scheduling, the BS periodically assigns fixed-size bandwidth grants to the SS. The bandwidth allocation process is regulated by two fixed parameters – Maximum Sustainable Traffic Rate (MSTR) and the maximum latency. The MSTR defines the peak data rate required by the application and the maximum latency determines the unsolicited grant interval which is the time between two successive UGS grants.

The IEEE802.16 standard also provides mechanism to synchronize the UGS data grant and packet transmission time using the FL (Frame Latency) and FLI (Frame Latency Indication) fields embedded in a grant management sub-header. Using these fields, the data transmission from the relays can be synchronized such that the relays from the i^{th} protection zone generates data at the x^{th} frame and the relays from $(i+1)^{\text{th}}$ zone generates data at the $(x+1)^{\text{th}}$ frame. This ensures minimum UGS delay by minimizing the time gap between packet generation and transmission.

In addition, WiMAX allows Persistent Scheduling technique that significantly reduces MAP signaling overhead for the UGS connections. Under persistent scheduling, the UL and DL burst information is sent once in a persistent MAP element and not repeated unless any parameter associated with the connection is changed[5].

C. Packet Loss and Retransmission

One of the key challenges of a wireless communications network is to prevent packet losses due to random noise and fading over a multi-path propagation environment. This is even more crucial for a differential protection scheme since the loss of a current measurement may significantly affect the accuracy and speed of the relaying operation. To recover the lost packets, WiMAX allows use of both Automatic Repeat Request (ARQ) and Hybrid Automatic Repeat Request (HARQ) retransmission schemes. However, since each current measurement has a small Time-To-Live (TTL) period, it is difficult to allow any retransmission since a measurement becomes obsolete after a new one is available.

Between ARQ and HARQ schemes, the HARQ is particularly suitable for a differential protection scheme. This is because, the ARQ relies on a feedback mechanism to detect a packet error and wait for a certain timeout parameter for the next retransmission opportunity. In contrast, the HARQ sends each data packet with Forward Error Correction (FEC) coding and the receiver uses both retransmitted packet and packet received with errors to reconstruct the original packet which reduces the number of retransmissions. Moreover, the HARQ scheme with Chase Combining (CC) provides fast retransmission opportunity through one of the dedicated Acknowledgment channels (ACK-CH) in the UL subframe (See Fig. 3).

Note that the overall packet delay including the retransmission attempts should remain below the current measurement

Table I: WiMAX PHY Parameters for the Capacity Analysis

Parameters	Notation	Values
Base Frequency	f_{sys}	2.3 GHz
Channel Bandwidth	BW	5 MHz
FFT Size	N_{FFT}	512
Sampling Factor	n	28/25
Sampling Frequency	$F_s = n * BW$	5.6 MHz
Subcarrier Spacing	$\Delta f = F_s/N_{FFT}$	10.94 KHz
Useful symbol time	$T_b = 1/\Delta f$	91.4 μs
Cyclic Prefix Time	T_g	$T_b/8$
OFDM Symbol Time	$T_s = T_b + T_g$	100.8 μs
Frame Duration	T_f	5 ms
Tx/Rx Transition Gap	T_{TTG}	106 μs
Rx/Tx Transition Gap	T_{RTG}	60 μs
No. of DL Data Subcarrier	$N_{sc}^{DL}(PUSC)$	360
No. of UL Data Subcarrier	$N_{sc}^{UL}(PUSC)$	272
UL:DL Ratio	r	1:1

interval since a measurement becomes obsolete once a new one is available. Hence, the maximum number of HARQ retransmissions should be limited to

$$R_{max} = \text{floor} \left(\frac{T - d_{max}}{\Delta t} \right). \quad (1)$$

where T is the current measurement interval, d_{max} is the maximum network delay and Δt is the minimum duration for a HARQ retransmission (i.e. one WiMAX frame for the HARQ with CC).

IV. CAPACITY ANALYSIS

In this section, we perform a basic capacity analysis of the WiMAX network in terms of number of differential relays that can be supported. We are particularly interested to see the effect of persistent scheduling and ROHC on the overall capacity and utilization of the network. For the capacity analysis, we assume a generic OFDMA/TDD based WiMAX network based on the IEEE802.16-2009 standard. A list of the key Physical layer (PHY) parameters used in the analysis is provided in Table I.

In an OFDMA based system, radio resources are allocated both in time and in frequency domain. The minimum possible data allocation unit is called an *OFDM symbol* which is comprised of a *Data Subcarrier* and an *OFDM Symbol-time*. Typically, data is allocated using a group of contiguous OFDM symbols called the *Subchannels*. Thus, each allocation can be visualized as rectangle with the number of OFDM symbols in the 'x' axis and the number of subchannels in the 'y' axis (see Fig. 3). The total number of OFDM symbol-times available in a WiMAX frame is given by

$$N_s = \text{floor} \left(\frac{T_f - T_{TTG} - T_{RTG}}{T_s} \right). \quad (2)$$

This yields a total 47 symbol-times for our assumed configuration in Table I. Since we assumed a UL/DL subframe ratio of 1:1, we allocate 24 symbols to the UL and 22 symbols to the DL (the first DL symbol time is used as

preamble) subframes. Hence, the number of OFDM symbol-times available in the UL is 6528 ($= N_{sc}^{UL} \times 24$) and in the DL is 7920 ($= N_{sc}^{DL} \times 22$).

As seen from Fig. 3, the DL subframe hosts the DL-MAP and the UL-MAP signaling messages. Each of these messages is comprised of a fixed header followed by a number of IEs. According to the IEEE802.16-2009 standard, a typical DL-MAP header size is 88 bits and IE size is 32 bits. On the other hand, a typical UL-MAP header size is 48 bits and IE size is 48 bits. Each UL-MAP message contains 3 fixed IEs for ranging and CQICH (Channel Quality Indication Channel) allocation areas (total 144 bits). Moreover, both DL and DL MAP messages are preceded by a WiMAX MAC header (48 bits). Thus, for an unloaded network (i.e. number of data IE=0), the total MAP message size is 336 bits (136 bits for DL-MAP and 240 bits for UL-MAP). Furthermore, the MAP messages are often sent with 2 or 4 repetition coding rate for increased robustness over the air-interface. Thus, assuming a repetition coding rate of 4, the total MAP message size is $(336 \times 4) = 1504$ symbols per frame. Therefore, the number of available data symbols in the DL subframe is $(7920 - 1504) = 6416$.

On the other hand, the UL subframe contains the initial ranging (IR) channel [6 subchannels x 1 symbol-times], bandwidth request (BR) ranging [6 subchannels x 2 symbol-times] and the CQICH [1 subchannel x 6 symbol-times] channel. Considering partial usage of subchannels (PUSC) in the UL, the number of data subcarriers in each subchannel is 16. Thus, the number of available data symbols in the UL subframe is $[6528 - (6 \times 1 \times 12 + 6 \times 2 \times 16 + 1 \times 6 \times 16)] = 6144$.

From Fig. 2, we see that the MPDU size of a current phasor packet is 58 bytes. However, the MPDU size can be further reduced by using an IP header compression techniques such as ROHC. WiMAX supports ROHC over both UL and DL data connections. For this study, we assume that the use of ROHC reduces the size of UDP/IP overhead to 6 bytes[10]. This yields a revised MPDU size of 36 bytes. Since each current measurement packet has a DL and a UL component, it requires both a DL and a UL MAP IE to be transported over the WiMAX network. Thus, the overall radio resource utilization of a current phasor packet over one WiMAX frame is given by

$$U = \frac{(MPDU + DL_{MAP})}{\text{No. of DL Symbols}} + \frac{(MPDU + UL_{MAP})}{\text{No. of UL Symbols}}. \quad (3)$$

Note that if persistent scheduling is used, both DL and UL signaling overheads become zero. Considering these two features along with the baseline configuration, Fig. 4 shows the overall utilization of a WiMAX frame supporting a single differential relay. Note that the actual resource utilization might be slightly higher than the one obtained by (3) due to the wastage of symbols during rectangular resource allocation in the OFDMA subchannels[5].

From Fig. 4, we see that the baseline configuration requires the highest radio resources among all. Also, the DL subframe utilization is higher than that of the UL. This is because, the DL subframe contains both DL and UL signaling components

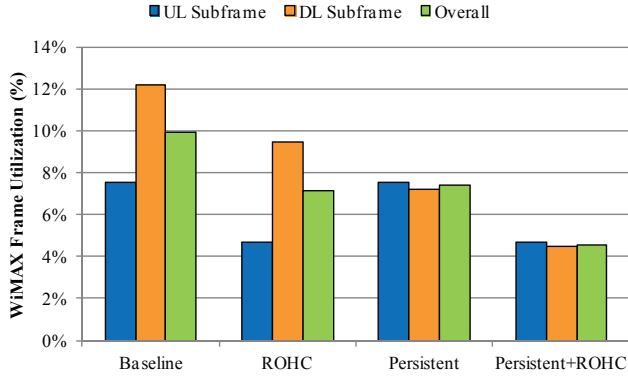


Figure 4: WiMAX Frame Utilization for one differential relay under different UGS configurations

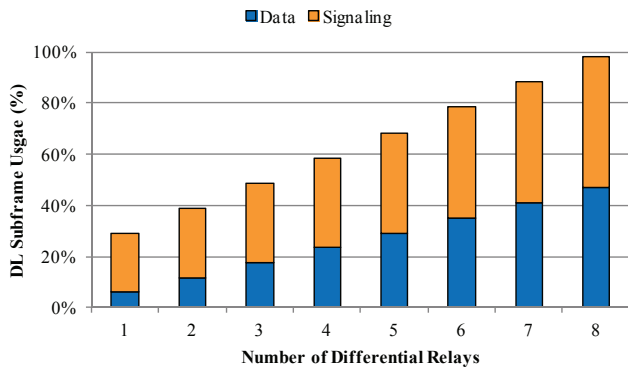


Figure 5: WiMAX DL subframe utilization at different number of relays under the baseline UGS configuration

which substantially takes up its available resources. This is further evident when the number of relays is increased for the baseline scenario as shown in Fig 5. Here, we see that as the number of relays increases, the signaling overheads increases at a higher rate than the data burst usage which in turn reduces the overall capacity of the frame.

Although the use of ROHC improves the UL frame utilization (see Fig. 4), the problem of higher DL subframe utilization still remains. This is solved when persistent scheduling is used which removes the signaling overheads associated with each packet. However, the best utilization is achieved when ROHC and persistent scheduling are used combinedly.

Now, the number of relays that can be supported by the WiMAX network is given by $Tota\ No.\ of\ Relays = No.\ of\ Relays\ per\ Frame * (T/T_f)$, where T_f is the WiMAX frame duration and T is the current measurement interval of the relays. Using this formula, we can find the total number of relays as shown in Fig.6.

V. PERFORMANCE ANALYSIS

To evaluate the delay and packet-loss performance of a LCDP scheme over a WiMAX network, we develop a single cell simulation model using the OPNET modeler 16.0. We use the same WiMAX PHY parameters as listed in Table I. The

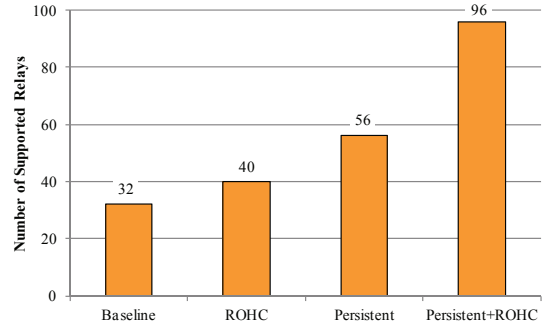


Figure 6: Number of supported relays under different UGS configurations (Current Measurement Interval = 20 ms)

Table II: Simulation Parameters

Parameters	Values
Physical Layer	OFDMA, TDD
Operating Frequency	2.3 GHz
Modulation Scheme	QPSK
FEC Type	$\frac{1}{2}$ rate CTC
Pathloss Model	Erceg, Type-B
BS Antenna height	32 m
SS Antenna height	1.5 m
SS Transmit Power	0.5 W
BS Transmit Power	5 W
BS Rx Sensitivity	-110 dBm
SS Rx Sensitivity	-95 dBm
Cell Radius	4 Km
Max. UGS Latency	20 ms
No. of HARQ Channels	8 (both UL/DL)
MAC Data Rate	1.22 Mbps (UL) 1.58 Mbps (DL)

rest of the key simulation parameters are listed in Table II. All the simulations are run for 5 minutes (60,000 WiMAX frames) to achieve a confidence level of 95%.

In the first simulation trial, we look into the delay performance of the LCDP scheme under the baseline UGS service with regular and synchronized grant allocation (described in Section III). We further vary the number of relays from 8 to 32 to examine its effect on the overall delay performance. The corresponding delay statistics are listed in Table III.

From the results, we see that under both UGS allocation modes, the WiMAX network is able to transfer the current phasors within the stipulated 20ms delay bound. However, grant synchronization significantly improves the UL delay while the DL delay remains the same. This is because, since the UGS grants are synchronized with the packet generation times, the relays are able to send their measurements immediately without any additional waiting period. This extra delay margin can be used to allow retransmissions in the network. Note that as the number of relays increase, the amount of delay increases for all cases. This is because, since the BS has to allocate data bursts in the UL/DL subframe over more OFDM symbol-times, a SS has to wait more to find its data grant.

In the next simulation trial, we examine the effect of packet-

Table III: WiMAX UGS Delay Statistics

(a) Regular UGS Grant				
No. of Relays	Uplink		Downlink	
	Mean	S.Dev.	Mean	S.Dev.
8	9.15	1.81	5.98	0.11
16	9.87	1.58	6.15	0.21
24	11.55	1.06	6.33	0.33
32	13.02	0.79	6.51	0.44

(b) Synchronous UGS Grant				
No. of Relays	Uplink		Downlink	
	Mean	S.Dev.	Mean	S.Dev.
8	5.01	1.48	5.98	0.11
16	5.04	1.48	6.15	0.21
24	5.06	1.48	6.33	0.33
32	5.08	1.48	6.51	0.44

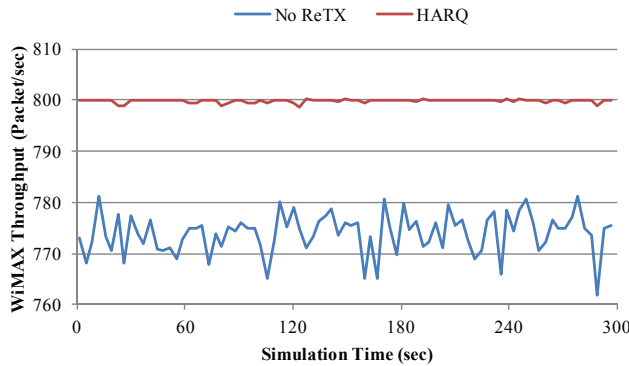


Figure 7: WiMAX network throughput for the LCDP scheme under no retransmission and HARQ retransmission

loss and retransmission on the network performance. The simulation scenario is comprised of 16 differential relays, each sending measurements using the baseline UGS service with synchronized grant. A log-normal fading of 5 dB was introduced in the network to simulate the effect of random packet loss in the system. From the previous results in Table III, we see that the end-to-end packet delay for such a configuration is around 11 ms (considering both UL and DL packet delay). Hence, to meet the delay bound of 20 ms, only one HARQ retransmission can be allowed as per (2). The corresponding throughput and delay performance of the WiMAX network is plotted in Fig. 7 and 8 respectively.

From the results, we see that the use of HARQ allows the WiMAX network to recover most of the lost packets. However, it increases the end-to-end packet delay due to the extra retransmission component (i.e. one WiMAX frame for this study). Nonetheless, it is acceptable since the end-to-end delay still remains below the required 20 ms bound.

VI. CONCLUSION

In this paper, we have examined the possible use of a WiMAX network for supporting differential protection

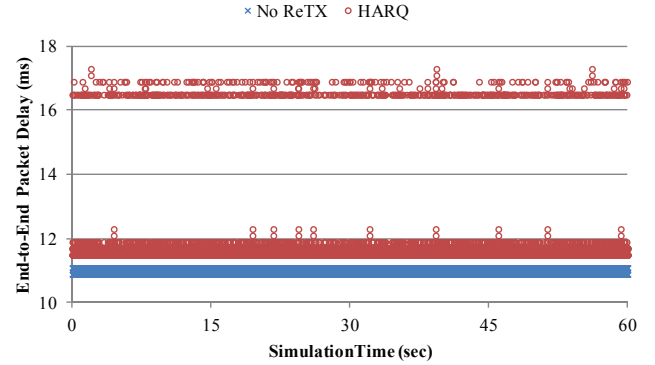


Figure 8: Distribution of packet delays for the LCDP scheme under no retransmission and HARQ retransmission (1 out of 5 minutes of simulation run-time).

schemes in the smart microgrids. Our analysis shows that the number of differential relays that can be supported by a WiMAX network can be tripped by the combined use of persistent scheduling and ROHC technique over the baseline UGS scheduling service. In addition, by synchronizing the current measurement time with the UGS allocation time, the WiMAX network can significantly improve the delay performance of the scheme. This additional delay margin can be used to allow a fast retransmission opportunity based on the chase-combining HARQ technique which may further improve packet-loss performance of the network.

The continuation of this work includes a joint performance analysis of the differential protection scheme by using a co-simulation model based on OPNET and a power system simulator. In addition, the use of a back-up protection schemes in case of link failures and/or increased packet-loss in the communications network also needs further investigation.

REFERENCES

- [1] S. Ward and T. Erwin, "Current differential line protection setting considerations," *RFL Electronics Inc.*, 2005.
- [2] M. Dewadasa, A. Ghosh, and G. Ledwich, "Protection of microgrids using differential relays," in *Universities Power Engineering Conference (AUPEC), 2011 21st Australasian*. IEEE, 2011, pp. 1–6.
- [3] T. S. Ustun, C. Ozansoy, and A. Zayegh, "Differential protection of microgrids with central protection unit support," in *IEEE Region Ten Conference (TENCON) Spring*, 2013.
- [4] "Transmission line protection principles," *GE Digital Energy*, 2007, available: <http://www.gedigitalenergy.com/>.
- [5] IEEE802.16-2009, *IEEE Standard for Local and metropolitan area networks Part 16: Air Interface for Broadband Wireless Access Systems*, pp. 1–2080, 2009.
- [6] H. Miller, J. Burger, N. Fischer, and B. Kasztenny, "Modern line current differential protection solutions," in *Protective Relay Engineers, 2010 63rd Annual Conference for*. IEEE, 2010, pp. 1–25.
- [7] A. G. Phadke and J. S. Thorp, *Synchronized phasor measurements and their applications*. Springer, 2008.
- [8] IEEE37.118.2-2011, *IEEE Standard for Synchrophasor Data Transfer for Power Systems*, pp. 1–53, 2011.
- [9] R. Khan and J. Khan, "Wide area pmu communication over a wimax network in the smart grid," in *Smart Grid Communications (SmartGrid-Comm), 2012 IEEE Third International Conference on*, 2012, pp. 187–192.
- [10] F. H. Fitzek, G. Schulte, E. Piri, J. Pinola, M. D. Katz, J. Huusko, K. Pentikousis, and P. Seeling, "Robust header compression for wimax femto cells," *WiMAX Evolution*, p. 185, 2009.